Global Gravity Field Model from Taiji-1

Liming Wu
Chang'an University
Peng Xu (xupeng@imech.ac.cn)
Chinese Academy of Sciences Institute of Mechanics https://orcid.org/0000-0002-3543-7777
Shuhong Zhao
Chang'an University
Li-E Qiang
National Space Science Center Chinese Academy of Sciences
Ziren Luo
Chinese Academy of Sciences Institute of Mechanics
Yueliang Wu
University of the Chinese Academy of Sciences

Research Article

Keywords: Taiji program, Gravity field recovery, Satellite gravity, Gravitational wave detection

Posted Date: March 31st, 2022

DOI: https://doi.org/10.21203/rs.3.rs-1463127/v1

Global Gravity Field Model from Taiji-1

Liming Wu[1,2], Peng Xu[2,3,4*], Shuhong Zhao[1], Li-E Qiang[5], Ziren Luo[2] and Yueliang Wu[6]

[1]Department of Geophysics, Chang'an University, Middle-section of Nan'er Huan Road, Xi'an, 710054, China.
[2]Institute of Mechanics, Chinese Academy of Sciences, No.15 Beisihuanxi Road, Beijing, 100190, China.
[3]Lanzhou Center of Theoretical Physics, Lanzhou University, No. 222 South Tianshui Road, Lanzhou, 730000, China.
[4]Hangzhou Institute for Advanced Study, University of Chinese Academy of Sciences, 84 Church Street SE, Hangzhou, 310024, China.
[5]National Space Science Center, Chinese Academy of Sciences, NO.1 Nanertiao Zhongguancun , Beijing, 100190, China.
[6]University of Chinese Academy of Sciences, No.19(A) Yuquan Road, Beijing, 100049, China.

*Corresponding author(s). E-mail(s): xupeng@imech.ac.cn;

Abstract

Taiji-1 is the first technology demonstration satellite of the Taiji program of China's space-borne gravitational wave antenna. After the demonstration of the key individual technologies, Taiji-1 continues collecting the data of the precision orbit determinations, the satellite attitudes, and the non-conservative forces exerted on the S/C. Therefore, during its free-fall, Taiji-1 can be viewed as operating in the high-low satellite-to-satellite tracking mode of a gravity recovery mission. In this work, one month data from Taiji-1's observations have been selected and the techniques are developed to resolve the long term interruptions and disturbances in the measurement data due to the scheduled technology demonstration experiments. The first global gravity model TJGM-r1911, that independently derived from China's own satellite mission, is successfully built from Taiji-1's observations. Compared with gravity models from CHAMP and other satellite gravity missions, the accuracy discrepancies exist, which is mainly caused by the data discontinuity problem.

As the approved extended free-falling phase with minimal disruptions and disturbances, Taiji-1 will serve as the first gravity mission satellite for China since 2022 and it will provide us the independent measurement of both the static and the monthly time-variable global gravity field.

Keywords: Taiji program, Gravity field recovery, Satellite gravity, Gravitational wave detection

1 Introduction

In 2000, Chinese Academy of Sciences (CAS) established China's first working group of the space borne gravitational wave (GW) observatories that led by Academician Wen-Rui Hu. China had then started her own journey to GW detection in space and joined the international corporations led by LISA [1]. Motivated mainly by the concept of ALIA mission [2],China's first space borne GW antenna mission concept was proposed in 2011 [3], and afterward, a conservative design was made [4, 5]. In 2016, the Adv-LIGO team announced the breaking news of the first detection of GW [6–9], which was soon recognized as one of the most significant achievements in this new century of general relativity. The subsequent GW observations by the LIGO-VIRGO collaboration raised the curtain of the new era of GW astronomy and astrophysics, and also boosted the progress of the space missions. Along with such breakthroughs, while being encouraged by the successful experiments of the LISA Pathfinder mission [10–14], the Taiji program in space was released by CAS in 2016 [15, 16], which outlined its 3-step R&D roadmap to China's space GW antenna in the future. The ultimate goal of the program is the Taiji mission, a heliocentric LISA-like mission to be launched in the early 2030s. Consisting of three space-crafts (S/C), the Taiji mission is an almost equilateral triangular constellation with the arm-length about 3×10^6 km and the sensitive band ranging from 0.1 mHz to 1 Hz. The scientific objectives will include such GW sources as coalescing super massive black hole binaries, extreme mass ratio inspirals, stochastic GW backgrounds and etc. [16–24].

As the first technology demonstration satellite of the Taiji program, Taiji-1 was approved by CAS in August 2018 and launched in August 2019. The most important individual technologies of China's space GW antenna were verified in space, including the gravitational reference sensors (GRS), the high precision laser interferometers, the drag-free control system, μ-N thrusters, the ultra-stable and clean platform and etc.. The successful operation of Taiji-1 has demonstrated and confirmed the designed performances of the scientific payloads and the satellite platform [20, 25]. During the final extended phase in 2022, the Taiji-1 satellite will carry out the challenging experiments on the global gravity recoveries.

During its scientific operation, Taiji-1 has continuously collected the precision orbit determination (POD) data based on the Global Navigation Satellite

Systems (GNSS), the satellite attitude data from star sensors, and also the precision measurements by the GRS of the non-conservative forces exerted on the S/C along its orbit. The orbital dynamics of Taiji-1 is determined by the forces acting on the S/C, which, due to their physical origins, can be divided into three categories: the gravitational forces including the almost centripetal force from the earth and the perturbations from the sun, the moon and other celestial bodies, the non-conservative forces from the space environments such as air drags, solar radiation pressure and the earth albedo, and also the disturbances from thruster events. Therefore, given the precision measurements of the satellite orbit and the non-conservative forces from both the space environments and the satellite propulsion, the detailed information of the earth gravitational field could be inferred based on the satellite dynamic model.

From this point of view, apart from the disruptions by the technology demonstration experiments such as the thruster performance tests, the drag-free control tests, the satellite maneuvers and so on, the free-falling mode of the Taiji-1 satellite can be viewed as the high-low Satellite-to-Satellite Tracking (hl-SST) mode of the earth gravity recovery mission [26–28]. See Fig. 1 for illustration.

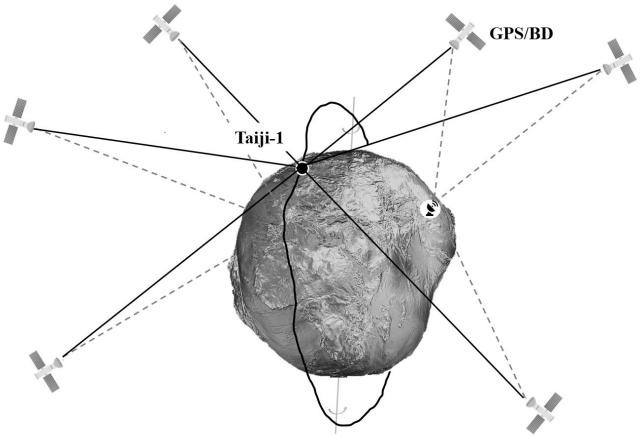

Fig. 1 The illustration of the high-low satellite-to-satellite tracking mode of Taiji-1.

Taiji-1 could then serve as the first gravity recovery satellite for China, which could provide us the independent measurements of both the static global gravity field over about one year and the monthly averaged time-variable gravity field of long wavelengths.

The gravity observations from Taiji-1, as the tentative data products, could then fuse with the up-coming geopotential measurements from the official Low-Low SST gravity recovery mission of China's satellite gravity program. Further, such precedent data products could also provide the opportunity to make valuable cross-validations between the two missions. Based on the idea, the

free-falling phase of Taiji-1 has been extended in the end of 2021, and the satellite are going to follow its geodesic orbit around the earth with minimal disruptions and disturbances only from the events like the attitude adjustments and etc..

In this work, we introduce the first earth gravity field achievement obtained from Taiji-1's observations during its science operation. The conventional energy integral method employed in gravity recoveries for hl-SST missions is outline in Sec. 2. Since the free-falling motion of the S/C in the earth gravitational field and the continual observations of the orbit and non-conservative forces are crucial to the global gravity recoveries, the data set is carefully selected to avoid the disruptions and gaps as much as possible. The measurement data from Taiji-1 and the ancillary models required are described in Sec. 3. While the interruptions and the anomalies still exist in the chosen data, the software package `TJGrav` is developed to resolve such problems and to process the data. The data fusion techniques are developed to synthesize the measurement data with certain models that are calibrated carefully by the measurements. The data processing procedure can be found in Sec. 4. At last, the first monthly earth gravity model `TJGM-r1911` independently derived from China's own satellite mission Taiji-1 is discussed in Sec. 5.

2 Energy integral method

Proposed by O'keefe in [29] firstly and investigated in detail in [30–33], the energy integral or the energy balance approach, has been developed as a full-fledged and widely used method in the global gravity inversions for hl-SST satellite gravity missions. It is based on the theoretical prediction that ideally the Jacobi's integral of a S/C motion is conserved along its orbits [34], which can be viewed as an equivalent to the conservation of total mechanical energy. Therefore, the balance between the kinetic energy and the gravitational energy of the S/C can be used to derive the detailed information of the gravity field, given the measured data of the S/C position and velocity.

The key to the approach in realistic applications is to account for the energy dissipation caused by the non-conservative surface forces acting on the S/C accurately. Generally, low earth orbits are adopted for the satellite gravity missions, and the main contributions to the total non-conservative force include the air drags, the solar radiation pressures and also the earth albedo pressure. One can use force models to reduce the errors caused by such energy loss, while the precise and real time measurements of such perturbation forces will greatly improve the fitting accuracy of the gravity field. Please see [26, 33, 35–38] for the detailed discussions of the energy integral method and its applications to the CHAMP, GRACE and GOCE missions.

Here, we outline the theoretical principle of the energy integral method and give the necessary definitions used in this work. The functional model chosen here to estimate the geopotential V is the following spherical harmonics series truncated at maximum degree N and defined in the earth centered spherical

coordinates system $\{r, \theta, \lambda\}$ (radius, geocentric latitude, longitude),

$$V(r,\theta,\lambda) = \frac{GM}{R}\left[1 + \sum_{n=2}^{N}\sum_{m=-n}^{n} A_{nm}\left(\frac{R}{r}\right)^{n+1} Y_{nm}(\theta,\lambda)\right], \tag{1}$$

where G is the gravitational constant, M the total mass of the earth, and R the mean equatorial radius. Y_{nm} denotes the surface spherical harmonics of degree n and order m

$$Y_{nm}(\vartheta,\lambda) = \bar{P}_{n|m|}(\sin\theta)\begin{cases}\cos m\lambda & m \geq 0\\ \sin|m|\lambda & m < 0,\end{cases} \tag{2}$$

where $\bar{P}_{nm}$ is the fully normalized associated Legendre function of degree n and order m, and $A_{nm} = \{C_{nm}, S_{nm}\}$, with C_{nm} for $m \geq 0$ and S_{nm} for $m \leq 0$, are the unknown spherical harmonic coefficients to be determined.

The earth gravity field, in terms of the geopotential coefficients A_{mn}, could be obtained from the least-squares solutions of the observation equations that link the orbit position and velocity solutions to the gravity field unknowns. The energy integral is used to derive the observation equations, which is defined along the S/C orbit

$$V = V_0 + \int_{t_0}^{t} \boldsymbol{g}\cdot\dot{\boldsymbol{r}}d\tau, \tag{3}$$

where V and V_0 are the earth geopotentials at the S/C orbit positions of time t and t_0 respectively, $\boldsymbol{r}$ and $\dot{\boldsymbol{r}}$ the position and velocity vector of the S/C in the earth-centered and earth-fixed (ECEF) reference frame. The vector $\boldsymbol{g}$ denotes the acceleration caused by static geopotentials of the earth

$$\boldsymbol{g} = \ddot{\boldsymbol{r}} + 2\boldsymbol{\omega}\times\dot{\boldsymbol{r}} + \boldsymbol{\omega}\times(\boldsymbol{\omega}\times\boldsymbol{r}) - \boldsymbol{a_{NC}} - \boldsymbol{a_G}, \tag{4}$$

where $\boldsymbol{\omega}$ is the angular velocity of the earth rotation. $\boldsymbol{a_{NC}}$ includes all the non-gravitational accelerations exerted by the satellite, and $\boldsymbol{a_G}$ counts for all the perturbations from other time-varying gravitational sources such as tides, the mass transfer in atmosphere and ocean, and the 3rd-body effect from the sun or the moon. To resolve the long wavelength or low-degree gravity field, we split the earth geopotentials into three parts U, V_l and V_h, where U represents the monople potential, V_l is the potential consisting of low-degree harmonics and V_h the one from high-degree harmonics. Thus, Eq.3 becomes

$$\begin{aligned} H + V_l(\boldsymbol{r}) =& \frac{1}{2}\dot{\mathbf{r}}\cdot\dot{\mathbf{r}} - \frac{1}{2}(\boldsymbol{\omega}\times\boldsymbol{r})\cdot(\boldsymbol{\omega}\times\boldsymbol{r}) \\ &- \int_{t_0}^{t}\boldsymbol{a_{NC}}\cdot\dot{\mathbf{r}}\mathrm{d}\tau - \int_{t_0}^{t}\boldsymbol{a_G}\cdot\dot{\mathbf{r}}\mathrm{d}\tau - U - V_h \end{aligned} \tag{5}$$

The unknowns integration constant H and the coefficients $\{C_{nm},\ S_{nm}\}$ of the low-degree components on the left-hand side of Eq. 5 are to be resolved

given the Taiji-1's observations and the modeled ancillary data substituted into the right-hand side of the equation.

3 data set and models

The Taiji-1 satellite was launched to a circular Sun-synchronous dawn/dusk orbit with the altitude about 600 km and inclination angle 97.67^o. The orbit has a stable sun-facing angle, which can provide a constant power supply for the battery and also the stable temperature gradient for the platform. The satellite is about 180 kg. With the orbit, the solar radiation pressure contributes to the non-conservative forces dominantly, and the air drags along the orbit turns out to be small. One of the key payloads of Taiji-1 is the GRS installed at the mass center of the S/C. Except for the drag-free control experiments during the science operation, where the satellite is controlled to trace the motions of the test mass (TM) inside the GRS along the radial direction, the GRS are set to work in the accelerometer mode in most cases. The electrostatic actuation forces keeping the TM to follow the motions of the S/C then give rise to the precise measurements of the non-gravitational forces exerted by the S/C.

The data products needed for the earth gravity recoveries include the POD data from both the GPS and BeiDou (BD) systems. GRS data of the non-gravitational forces measured in the Satellite Frame (SF) and S/C attitude data transform the physical measurements from SF to the inertial reference frame. In this work, our first Taiji-1 gravity model is based on the data from 01-11-2019 to 31-11-2019. As mentioned, during this month few experiments related to the GRS, the thrusters, and the satellite-maneuvers were performed. The S/C maintained steadily in the earth pointing attitude and the POD data in good quality. The length of data was determined because the extension could hardly improve the final fitting accuracy due to the frequent disruptions and gaps in the data from the technology demonstration experiments. Further, since the monthly measurements of the time-variable gravity field from Taiji-1's extended free-falling phase is under preparation, this first monthly gravity model could serve as a reference.

Orbits. The orbit precision of Taiji-1 is determined by the GNSS, including both the GPS and the BD system. The POD data from GPS and BD are both defined in the ECEF frame with the sampling rate of 1 Hz. The amplitude spectrum density (ASD) of the POD data including the positions and the velocities of Taiji-1 in the ECEF frame is shown in Fig. 2. In most cases, the Taiji-1 satellite can be more often tracked by GPS satellites than by the BD satellites. Fig. 3 shows the difference between the measurements from BD and GPS.

Attitude. The S/C attitude is measured by star sensors, and the detailed information of how to rotate from the satellite frame to the inertial frame is provided by the Euler angle $\{\theta,\ \phi,\ \psi\}$ data product. In Fig. 4 the time series of the S/C attitude on 01-11-2019 are shown. One could see the large variations

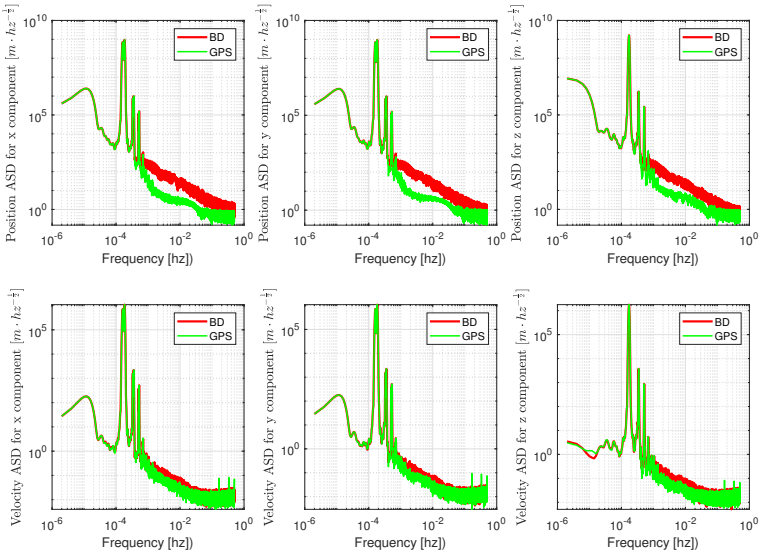

Fig. 2 ASDs of Taiji-1's POD data from both GPS and BD in the ECEF frame.

with the orbital period along the pitch axis (y-axis in the SF). The rotation matrices for each axis are given by

$$\mathbf{R}_x(\theta) = \begin{pmatrix} 1 & 0 & 0 \\ 0 & \cos\theta & \sin\theta \\ 0 & -\sin\theta & \cos\theta \end{pmatrix} \tag{6}$$

$$\mathbf{R}_y(\phi) = \begin{pmatrix} \cos\phi & 0 & -\sin\phi \\ 0 & 1 & 0 \\ \sin\phi & 0 & \cos\phi \end{pmatrix} \tag{7}$$

$$\mathbf{R}_z(\psi) = \begin{pmatrix} \cos\psi & \sin\psi & 0 \\ -\sin\psi & \cos\psi & 0 \\ 0 & 0 & 1 \end{pmatrix} \tag{8}$$

The total transformation matrix from the inertial reference frame to the SF frame reads

$$\boldsymbol{R} = \boldsymbol{R}_x \boldsymbol{R}_y \boldsymbol{R}_z \tag{9}$$

Non-conservative forces. The non-conservative forces are measured by the GRS in the accelerometer mode. The sensor unit of the electrostatic GRS on-board Taiji-1 contains two parts: the mechanical assembly and the front-end electronics unit (FEE). The mechanical assembly consists of a 72 g parallel hexahedral titanium alloy TM and an electrode cage that encloses the TM. The TM, as the inertial reference, is suspended electrostatically inside the cage. When non-gravitational forces on the S/C cause the relative motions between

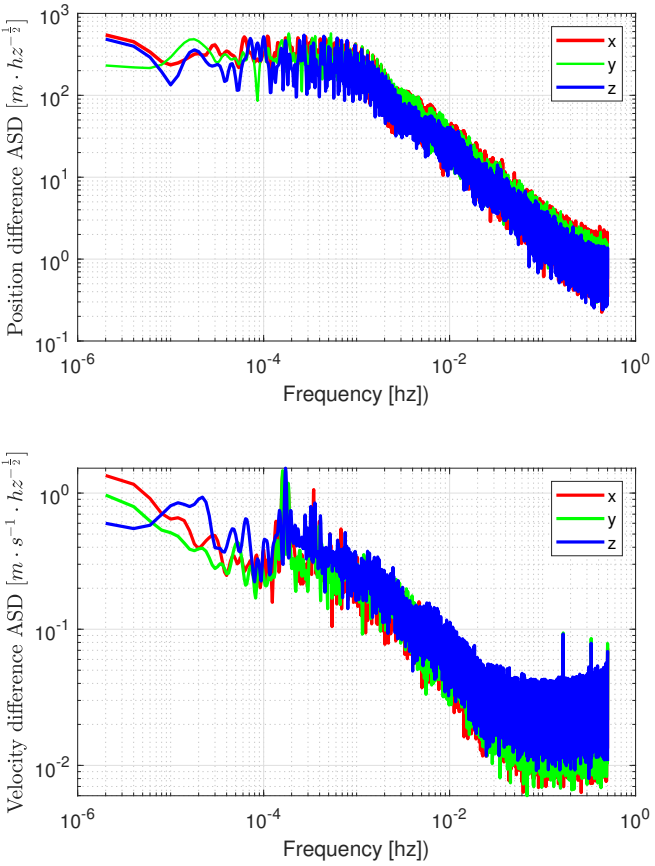

Fig. 3 ASDs of the POD data differences between BD and GPS in the ECEF frame.

the TM and the cage, the capacitance between the TM and the electrodes changes slightly and induces signals that could be picked up by the FEE. Based on the position sensor data, the TM maintained its nominal position inside the cage by applying low frequency actuation voltages through the electrodes. The voltages sampled at 100 Hz are then transformed, with the calibrated bias and the scale factors, into the non-conservative accelerations exerted by the S/C in the SF.

The sensitivities of the three GRS axes are different. The two high sensitive axes, y and z axes, are along the flight direction and the orbital normal direction respectively while the sensitivity of x-axis is low which is parallel to the radial direction or the earth pointing direction. According to the in-orbit performance tests [25, 39, 40], the resolutions of the high sensitive axes reach the level of $10^{-10}\mathrm{m}/s^2/\mathrm{Hz}^{1/2}$ in the frequency band from 0.01 Hz to 1 Hz

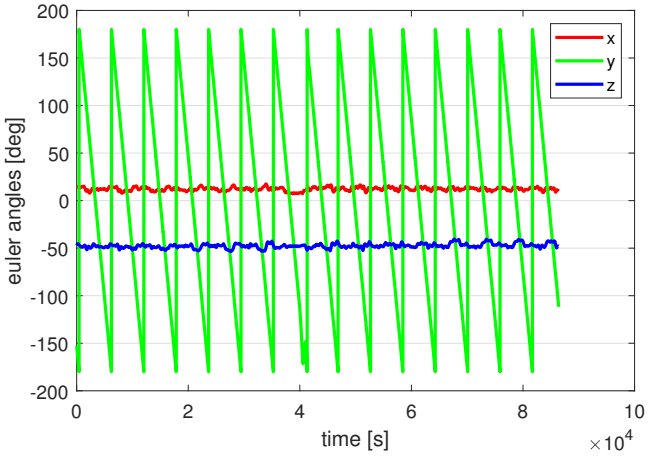

Fig. 4 Time series of the S/C attitude data (Euler angles) on 01-11-2019

and $10^{-9} m/s^2/Hz^{1/2}$ in the low frequency band from 0.1 mHz to 0.01 Hz. It will provide us the faithful measurements of the non-gravitational accelerations along Taiji-1's orbit, according to the known force models. See Fig. 8 in the next section. Fig. 5 shows the ASDs of the measured non-gravitational accelerations in the SF frame.

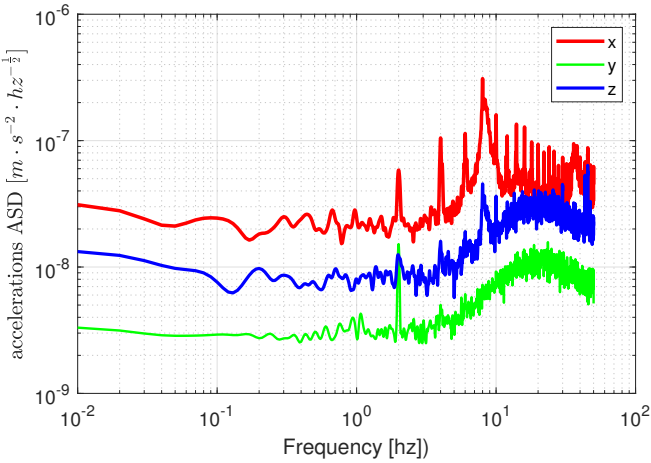

Fig. 5 ASDs of the measured non-gravitational accelerations in the SF frame.

Table 1 Models for the perturbation forces

Perturbation	Model	Maximum degree
earth's gravity field	EGM2008	degree/order 100
Dealiasing	GRACE AOD1B RL06	degree/order 50
Ephemerides of Sun and Moon	JPL DE421	
Solid earth tides	IERS2010	degree/order 4
Relativistic corrections	IERS2010	
Atmospheric density	NRLMSISE-00	
earth Albedo	CERES	

3.1 Ancillary models

To determine the long wavelength and low-degree gravity field model, the interference from the high-degree geopotentials, the tidal signals and the 3rd-body perturbations, needs to be suppressed or removed. In this work, the EGM2008 model [41] is employed as the prior gravity model, and the reference to assess and validate our Taiji-1 gravity model. Solid-earth tides and the relativistic corrections are also considered according to the standard IERS2010 [42]. The 3rd-body perturbations from the sun and the moon are included, and the required position and the velocity vectors of the sun and the moon are obtained from JPL's ephemerids DE421 [43]. The non-tidal atmospheric and oceanic mass variations are evaluated based on the atmosphere and ocean dealiasing product AOD1B RL06 [44].

As mentioned, there are disruptions and gaps in the selected data, especially in the measurements of the GRS system. Therefore, the simulations of the non-gravitational forces calibrated and adjusted by the measurements along the orbits will be employed as the complementary data when the disturbances or the long term interruptions happen. In this work, the atmospheric density model NRLMSIS-00 [45] and earth albedo model CERES [46, 47] are used.

The full list of all the models used can be found in Table 1.

4 Data processing

The software package `TJGrav` developed in this work for Taiji-1's gravity field modeling contains three main sub-modulars: the data `Pre-Processor`, the `SST-Processor`, and the `Solver`. Please see Fig. 6 for the architecture of `TJGrav` and the flow chart of the data processing procedure.

Common manipulations including the data quality check, the identifications of gaps and gross errors, adding flags, the anomalies removing and replaced with interpolations, data smoothing, anti-aliasing and down-samplings are carried out by the `Pre-processor.`

Take the key POD data as an example. The quality of the data are generally good, but there are still gaps and outliers. The search for the anomalies is executed in the first place. To make sure the continuity of the POD data in the observation equation 5, the outliers and the gaps are replaced or filled up with values evaluated in terms of the Fourier least-square-fitting method.

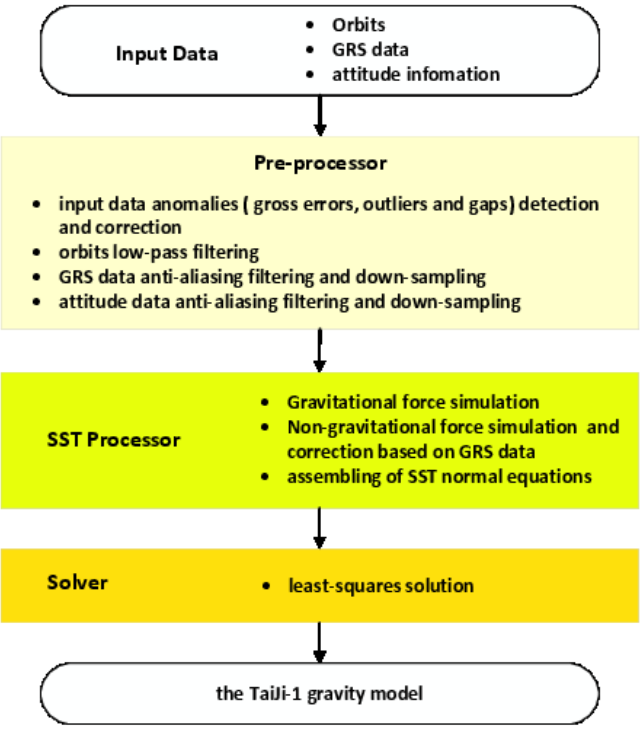

Fig. 6 Software architecture of `TJGrav` and the flow chart of the data processing procedure.

The replaced data will not be used to establish the normal equations, but only to calculate the integration in the observation equation 5. In the high frequency band of the POD data, the Signal to Noise Ratio of the orbital perturbations from geopotentials decreases. Therefore, to suppress the high frequency noises a low-pass filter at 0.005 Hz is imposed. After this, the POD data is down-sampled from 1 Hz to 0.2 Hz. The similar processing is applied to the original GRS data and S/C attitude data, and after a certain smoothing and anti-aliasing filtering they are also down-sampled to 0.2 Hz before use.

In the `SST-Processor`, we gather all the needed ancillary data, which are either obtained from the numerical simulations based on well-tested models or official data products released. Afterward, the normal equation is established and ready to export to the `Solver`.

Required gravitational perturbations from other sources are modeled and calculated in the ECEF frame. As mentioned in the previous sections, the required data include perturbations from the 3rd-body (the sun and the moon), solid-earth tides, AOD, and also the relativistic corrections. In the ECEF frame, the perturbation forces due to the 3rd-body is modeled as

$$\boldsymbol{a}_{\text{sun}} = -GM_{sun}\left(\frac{\boldsymbol{l}_{\text{sun}}}{|\boldsymbol{l}_{\text{sun}}|^3} + \frac{\boldsymbol{r}_{\text{sun}}}{|\boldsymbol{r}_{\text{sun}}|^3}\right)$$

$$\boldsymbol{a}_{\text{moon}} = -GM_{\text{moon}}\left(\frac{\boldsymbol{l}_{\text{moon}}}{|\boldsymbol{l}_{\text{moon}}|^3} + \frac{\boldsymbol{r}_{\text{moon}}}{|\boldsymbol{r}_{\text{moon}}|^3}\right)$$

where M_{sun} and M_{moon} are the masses of the sun and the moon, $\boldsymbol{l}_{\text{sun}}$, $\boldsymbol{l}_{\text{moon}}$ are the position vectors of the S/C relative to the sun and moon, and $\boldsymbol{r}_{\text{sun}}$, $\boldsymbol{r}_{\text{moon}}$ the position vectors of the earth relative to the sun and the moon. Please see Fig. 7 for the simulated gravitational perturbations on 01-11-2019.

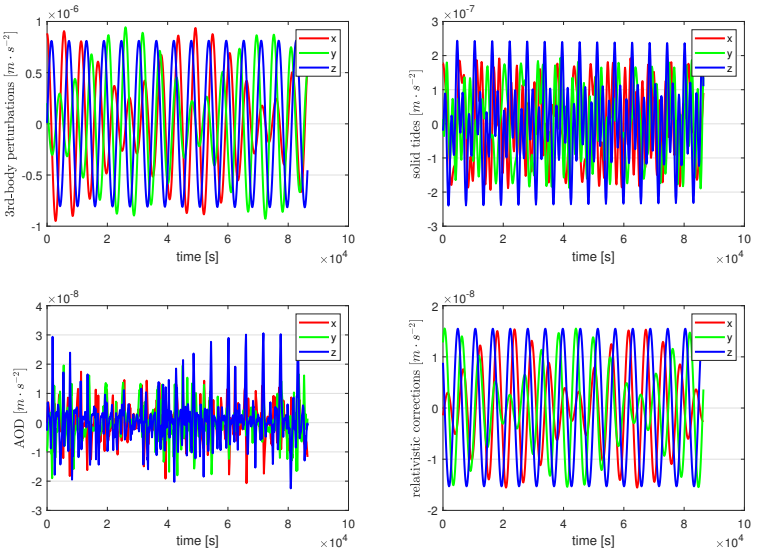

Fig. 7 Time series of the simulated gravitational perturbations in ECEF frame on 01-11-2019.

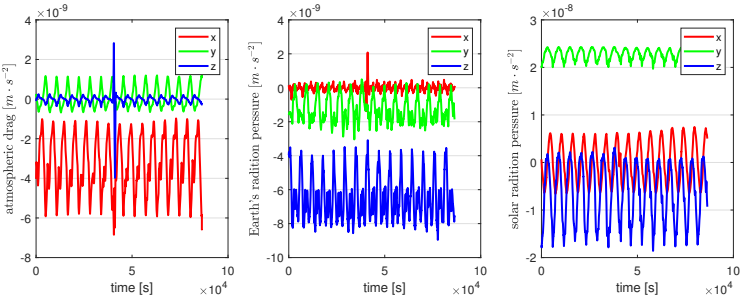

Fig. 8 Time series of the simulated non-gravitational forces in ECEF frame on 03-11-2019

The resolution power of the GRS on-board Taiji-1 ($\sim 10^{-10} m/s^2/Hz^{1/2}$) makes it sensible to the small disturbances occurred on the platform. The TM, as the inertial reference, couples to the surrounding physical fields in complicated ways. The events like the temperature variations of the sensor unit, the slight mechanical vibrations of the platforms and so on may cause the fake signals in the GRS measurements. The transient data anomalies of those kinds can be fixed by the `Pre-Processor`. However, the continuous attitude adjustments with the momentum wheels, the orbital maneuvers and certain experiments involving the GRS or the thrusters may cause the long term interruptions in the data. During the time, the modeled data of the non-gravitational forces are needed to fuse with the GRS measurements in order to complete the missing pieces.

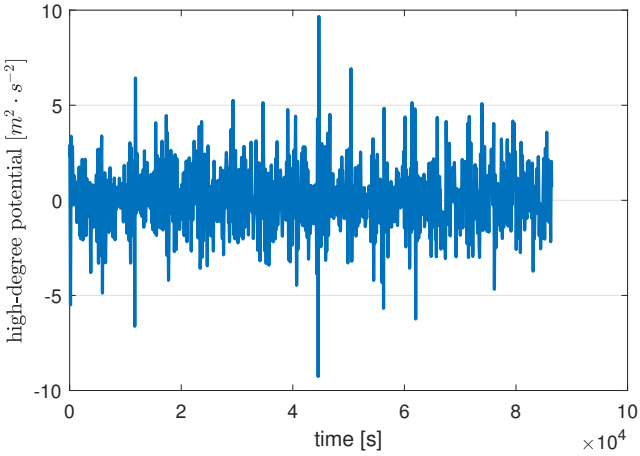

Fig. 9 Time series of the simulated high-degree geopotentials of degree/order from 21 to 100 on 01-11-2019.

As discussed in Sec. 3, the air-drag is modeled as

$$\boldsymbol{a}_{drag} = -\frac{1}{2}\rho \frac{C_D A}{m_{SC}} \boldsymbol{v}_{rel}^2 \frac{\boldsymbol{v}_{rel}}{|\boldsymbol{v}_{rel}|} \tag{10}$$

where ρ is the air density, C_D is the drag coefficient ($C_D = 2.2$), m_{SC} is the mass of the satellite, $\boldsymbol{v}_{rel}$ the velocity of the satellite relative to air, and A is the windward area of the satellite. The radiation pressure either from the solar radiation or the earth albedo is modeled as

$$\boldsymbol{F} = \sum_i^n \boldsymbol{E} \frac{A_i \cos\theta}{c\, m_{SC}} \left[(1-\eta)\, \hat{\boldsymbol{E}} + 2\eta \cos\theta \hat{\boldsymbol{n}} \right] \tag{11}$$

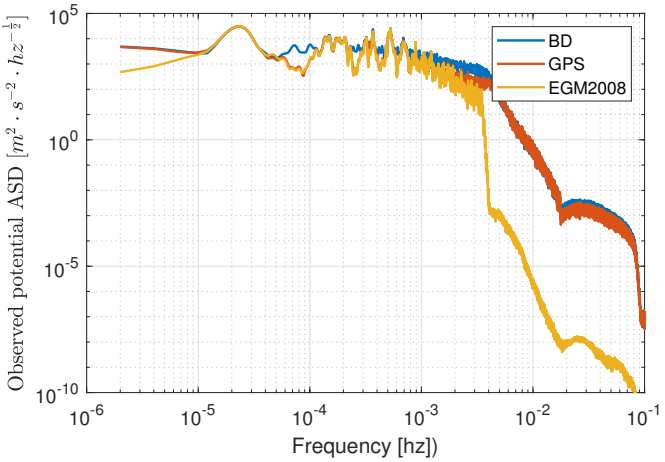

Fig. 10 ASDs of the observed low-degree potential without the C_{20} term.

where $\boldsymbol{E}$ is the radiation flux, A_i and $\hat{\boldsymbol{n}}$ denote the area and the normal direction of the S/C surface i, η the fraction of the incoming radiation that is reflected by the surface i, and θ the angle between $\boldsymbol{E}$ and $\hat{\boldsymbol{n}}$. The key parameters in the above equations, the drag coefficient and the reflection coefficient, depend on the physical properties of the S/C surfaces and the real-time status of the surrounding environments, and may also change with time. Therefore the modeled data is compared with the GRS measurements to adjust the parameters. In Fig. 8, we calibrate the simulated non-gravitational forces by the measured data from 01-11-2019. The magnitude of the simulated atmospheric drag is smaller than that of the solar radiation pressure because of the 600 km altitude. In addition, one could also see that the averaged solar radiation pressure along the pitch-axis (y-axis) of the SF frame is the largest, since $\hat{\boldsymbol{y}}$ is the orbital normal direction oriented to the sun.

Last but not the least, the high-degree geopotentials of degree/order from 21 to 100 along the Taiji-1's orbit are simulated based on EGM2008. See Fig. 9 for the illustration.

Given all the processed measurement data and the modeled ancillary data so far, the observed low-degree earth geopotentials along the orbit is solved by the `SST-Processor` based on the observation equation 5. In Fig. 10, the ASDs of the observed low-degree potentials along the orbit from both the BD and GPS measurements are compared with that from the EGM2008 model. It is found that the observations from the GPS agrees with the EGM2008 model to a large extent.

Finally, in the `Solver` sub-modular, the normal equations based on Eq. 1 are constructed in the form

$$\boldsymbol{A}\boldsymbol{x} = \boldsymbol{b} \tag{12}$$

where $\boldsymbol{b}$ is the observation vector, $\boldsymbol{x}$ is consist of the unknown geopotential coefficients, and $\boldsymbol{A}$ the design matrix. The global gravity model is obtained

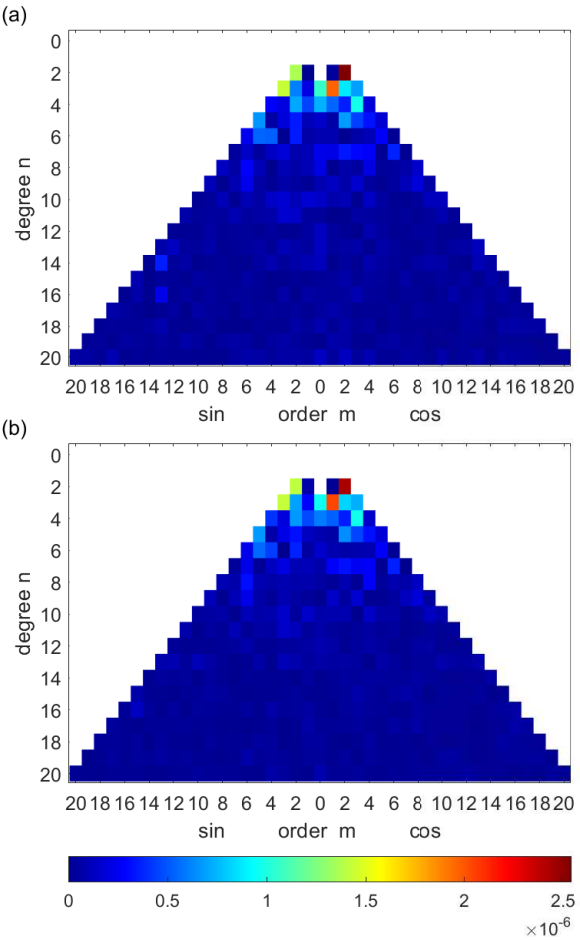

Fig. 11 Geopotential coefficients of the Taiji-1's gravity filed model `TJGM-r1911` with the C_{20} term removed: (a)BD; (b)GPS.

in terms of the least-square solutions of the above normal equations, applying the Cholesky reduction method

$$\boldsymbol{x} = \left(\boldsymbol{A}^{\top}\boldsymbol{A}\right)^{-1}\boldsymbol{A}^{\top}\boldsymbol{b}. \tag{13}$$

5 Results and conclusions

We have obtained the first monthly global gravity model from Taiji-1's observations based on the measurements in November 2019. The geopotential data product, denoted as `TJGM-r1911`, is now archived by the Taiji-1 data processing center of CAS at Beijing, and it will be released soon together with the new monthly data products derived from the much better observations during

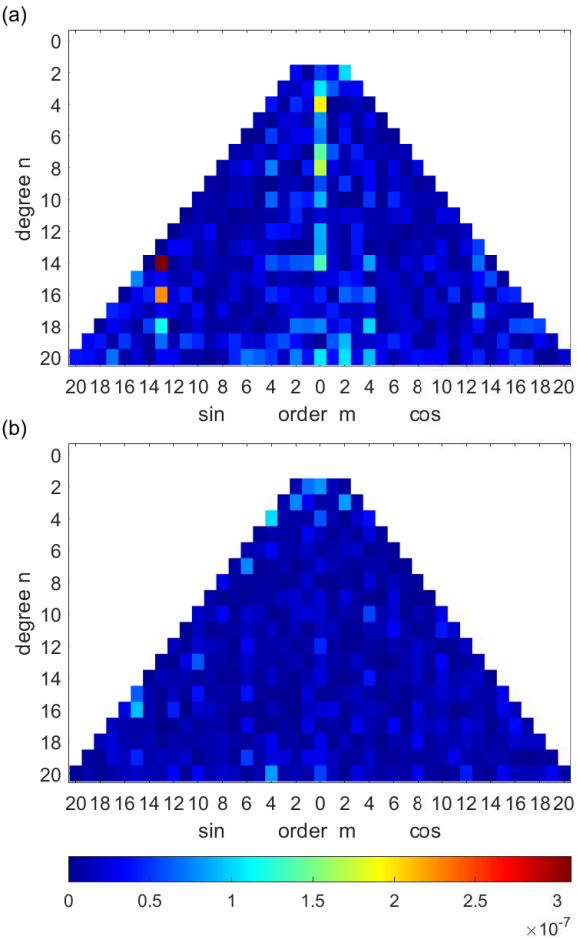

Fig. 12 Differences between the Taiji-1 gravity model `TJGM-r1911` and EGM2008: (a)BD; (b)GPS.

Taiji-1's extended free-falling phase in this year. These data products contain the geopotentials coefficients of spherical harmonics up to certain degree $\{C_{nm},\ S_{nm}\}$ and the variances $\{\Delta C_{mn},\ \Delta S_{nm}\}$.

As mentioned previously, mainly because of the long term interruptions in the observation data, as well as the rather high orbit attitude of Taiji-1, our first product `TJGM-r1911` is truncated at the 20th degree. To make the cross check and comparisons, `TJGM-r1911` also contains two independent sets of the geopotential data obtained from the GPS's and BD's observations respectively. Please see Fig. 11 and Fig. 12 for the comparisons. The differences can be seen clearly in the plots in Fig. 13, Fig. 14 and Fig. 15. The gravity model from BD observations shows larger deviations from the EGM2008 model than that from the GPS observations.

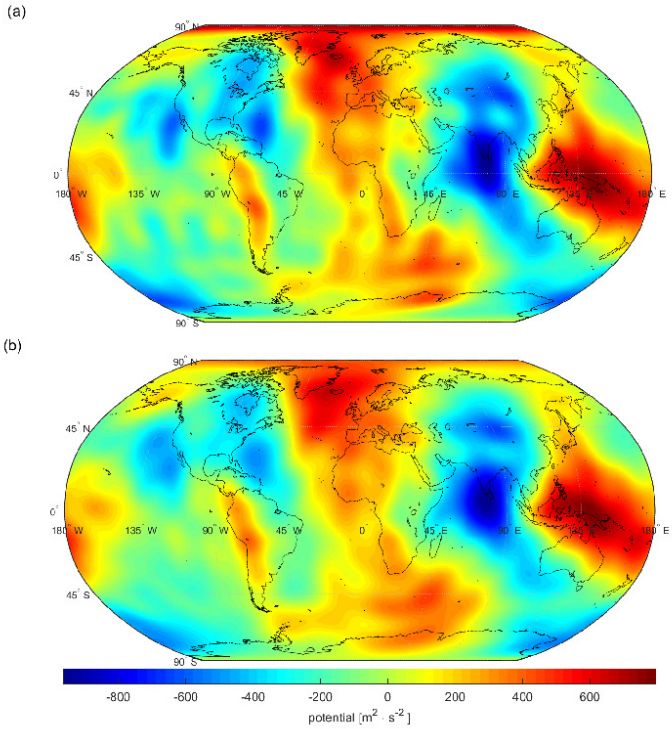

Fig. 13 Geopotentials of the Taiji-1 gravity model `TJGM-r1911`: (a)BD; (b)GPS.

Also, in Fig. 15, the degree Root Mean Square (RMS) degree is estimated from the prior reference model $\{C^P_{nm},\ S^P_{nm}\}$

$$RMS_n = \sqrt{\frac{\sum_{m=0}^{n}\left(C_{nm}-C^P_{nm}\right)^2+\sum_{m=1}^{n}\left(S_{nm}-S^P_{nm}\right)^2}{2n+1}}, \qquad (14)$$

the deviations of the `TJGM-r1911` model from the EGM2008 model turns out to be larger than those from similar hl-SST missions. Compared with the gravity models from the CHAMP mission [27, 35–37, 48–51], the degree RMS of our `TJGM-r1911` model is about one order of magnitude worse than that of the CHAMP models, depending on the used methods and ancillary data. The poor degree RMS comes from two factors. First, the Taiji-1's orbit has a large inclination angle, and the altitude ($\sim$ 600 km) is higher than all the gravity recovery satellites ever launched. The inclination causes signals loss in the high latitude areas, and the higher altitude gives rise to the magnitudes of the geopotentials at the orbit to decrease. Second, as already mentioned, the data is from the window period of the science operation phase, even though the data set is carefully selected, there still exist long interruptions and large disturbances, especially those for the key GRS measurements of the non-gravitational forces. The techniques such as data fusions with the calibrated simulations are

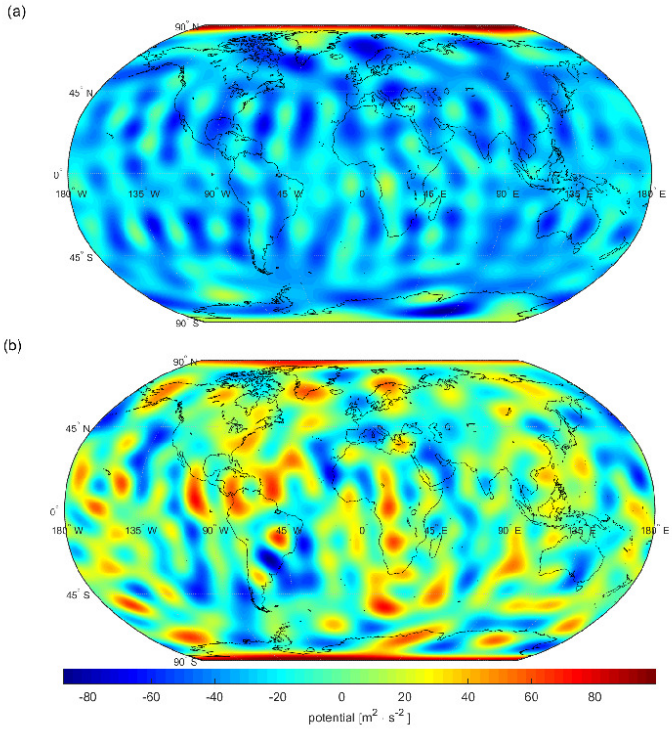

Fig. 14 Geopotential differences between the Taiji-1 gravity model `TJGM-r1911` and EGM2008: (a)BD; (b)GPS.

employed to improve the fitting accuracy. However, the problem of the data quality and the discontinuity are believed to be the key reasons to the increased errors, which will be greatly improved in the extend free-falling phase of Taiji-1 this year.

Conclusions. Gravity field is one of the fundamental physical fields of a planet. For Earth, the global gravity field contains vast amount of valuable information about the mass distributions and transfers on the earth surface, the global climate changes, the groundwater storage, the earth internal activities and so on. Great efforts has been paid in the satellite gravity, and after the CHAMP, GRACE, GOCE, and GRACE FO missions, the next generation gravity missions with advanced technologies including relativistic measurements are under investigations.

In this work, we carefully select the data of one month from Taiji-1's observations, and develop the data fusion techniques to resolve the problem of the long term interruptions and the disturbances in the measurements caused by the scheduled technology demonstration experiments. The first global gravity model `TJGM-r1911` independently derived from China's own satellite mission is then successfully produced from the Taiji-1's observations. The existed discrepancies between the first global gravity model `TJGM-r1911` and the gravity

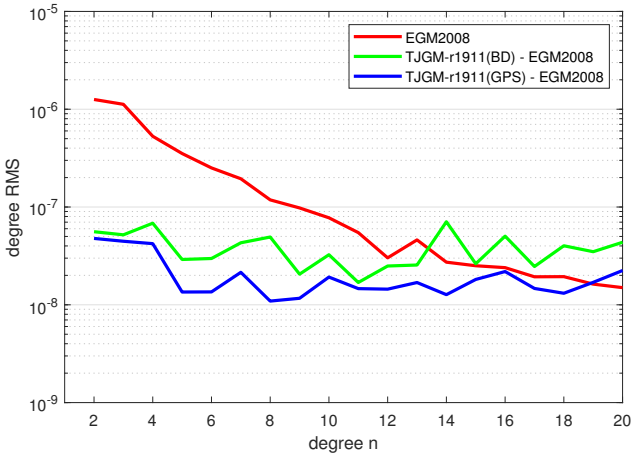

Fig. 15 Degree RMS of the Taiji-1 gravity model from the EGM2008 model.

models from CHAMP or other hl-SST missions are mainly caused by the data quality discontinuity problems. The capability of the Taiji-1 satellite serving as a fully-functional hl-SST satellite gravity mission for China has been demonstrated and confirmed. The extended free-falling phase of Taiji-1 with minimal disruptions and disturbances has been approved to be started this year. With the techniques developed in this work, Taiji-1 could serve as the first satellite gravity mission for China, which could provide us independently both the static mappings of global gravity field and monthly averaged measurements of the time-variable gravity field.

Acknowledgments. This work is supported by the National Key Research and Development Program of China No. 2020YFC2200601 and No. 2020YFC2200104, the Strategic Priority Research Program of the Chinese Academy of Sciences Grant No. XDA15020700, and the Youth Fund Project of National Natural Science Foundation of China No. 11905017.

Declarations

Conflict of Interest The authors have no competing interests to declare that are relevant to the content of this article.

References

[1] Danzmann K. LISA Revealing a hidden Universe. European Space Agency; 2011.

[2] Bender PL. Additional astrophysical objectives for LISA follow-on missions. Classical and Quantum Gravity. 2004 Mar;21(5):S1203–S1208. https://doi.org/10.1088/0264-9381/21/5/120.

[3] Gong X, Xu S, Bai S, Cao Z, Chen G, Chen Y, et al. A scientific case study of an advanced LISA mission. Classical and Quantum Gravity. 2011 May;28(9):094012. https://doi.org/10.1088/0264-9381/28/9/094012.

[4] Gong X, Lau YK, Xu S, Amaro-Seoane P, Bai S, Bian X, et al. Descope of the ALIA mission. Journal of Physics: Conference Series. 2015 May;610:012011. https://doi.org/10.1088/1742-6596/610/1/012011.

[5] Xue-fei G, Sheng-nian X, Ye-fei Y, Shan B, Xing B, Zhou-jian C, et al. Laser Interferometric Gravitational Wave Detection in Space and Structure Formation in the Early Universe. Chinese Astronomy and Astrophysics. 2015 Oct;39(4):411–446. https://doi.org/10.1016/j.chinastron.2015.10.001.

[6] The LIGO Scientific Collaboration, Aasi J, Abbott BP, Abbott R, Abbott T, Abernathy MR, et al. Advanced LIGO. Classical and Quantum Gravity. 2015 Apr;32(7):074001. https://doi.org/10.1088/0264-9381/32/7/074001.

[7] Abbott BP, Abbott R, Abbott TD, Abernathy MR, Acernese F, Ackley K, et al. Observation of Gravitational Waves from a Binary Black Hole Merger. Physical Review Letters. 2016 Feb;116(6):061102. https://doi.org/10.1103/PhysRevLett.116.061102.

[8] Abbott BP, Abbott R, Abbott TD, Abernathy MR, Acernese F, Ackley K, et al. Observing gravitational-wave transient GW150914 with minimal assumptions. Physical Review D. 2016 Jun;93(12):122004. https://doi.org/10.1103/PhysRevD.93.122004.

[9] Abbott BP, Abbott R, Abbott TD, Abernathy MR, Acernese F, Ackley K, et al. Properties of the Binary Black Hole Merger GW150914. Physical Review Letters. 2016 Jun;116(24):241102. https://doi.org/10.1103/PhysRevLett.116.241102.

[10] Armano M, Audley H, Auger G, Baird JT, Bassan M, Binetruy P, et al. Sub-Femto- g Free Fall for Space-Based Gravitational Wave Observatories: LISA Pathfinder Results. Physical Review Letters. 2016 Jun;116(23):231101. https://doi.org/10.1103/PhysRevLett.116.231101.

[11] Armano M, Audley H, Baird J, Binetruy P, Born M, Bortoluzzi D, et al. Beyond the Required LISA Free-Fall Performance: New LISA Pathfinder Results down to 20 μ Hz. Physical Review Letters. 2018 Feb;120(6). https://doi.org/10.1103/PhysRevLett.120.061101.

[12] Armano M, Audley H, Baird J, Binetruy P, Born M, Bortoluzzi D, et al. LISA Pathfinder platform stability and drag-free performance. Physical Review D. 2019 Apr;99(8):082001. https://doi.org/10.1103/PhysRevD.

99.082001.

[13] Armano M. LISA_Pathfinder. arXiv. 2019;p. 1903.08924. https://doi.org/10.1142/9789811207402_0013.

[14] Anderson G, Anderson J, Anderson M, Aveni G, Bame D, Barela P, et al. Experimental results from the ST7 mission on LISA Pathfinder. Physical Review D. 2018 Nov;98(10):102005. https://doi.org/10.1103/PhysRevD.98.102005.

[15] Cyranoski D. Chinese gravitational-wave hunt hits crunch time. Nature. 2016 Mar;531(7593):150–151. https://doi.org/10.1038/531150a.

[16] Hu WR, Wu YL. The Taiji Program in Space for gravitational wave physics and the nature of gravity. National Science Review. 2017 Sep;4(5):685–686. https://doi.org/10.1093/nsr/nwx116.

[17] Ruan WH, Guo ZK, Cai RG, Zhang YZ. Taiji program: Gravitational-wave sources. International Journal of Modern Physics A. 2020 Jun;35(17):2050075. https://doi.org/10.1142/S0217751X2050075X.

[18] Luo Z, Wang Y, Wu Y, Hu W, Jin G. The Taiji program: A concise overview. Progress of Theoretical and Experimental Physics. 2020 Jul;p. ptaa083. https://doi.org/10.1093/ptep/ptaa083.

[19] Luo Z, Guo Z, Jin G, Wu Y, Hu W. A brief analysis to Taiji: Science and technology. Results in Physics. 2020 Mar;16:102918. https://doi.org/10.1016/j.rinp.2019.102918.

[20] The Taiji Scientific Collaboration, Wu YL, Luo ZR, Wang JY, Bai M, Bian W, et al. Taiji program in space for gravitational universe with the first run key technologies test in Taiji-1. International Journal of Modern Physics A. 2021 Apr;36(11n12):2102002. https://doi.org/10.1142/S0217751X21020024.

[21] Ruan WH, Liu C, Guo ZK, Wu YL, Cai RG. The LISA–Taiji network. Nature Astronomy. 2020 Feb;4(2):108–109. https://doi.org/10.1038/s41550-019-1008-4.

[22] Ruan WH, Liu C, Guo ZK, Wu YL, Cai RG. The LISA-Taiji Network: Precision Localization of Coalescing Massive Black Hole Binaries. Research. 2021 Jan;2021:1–7. https://doi.org/10.34133/2021/6014164.

[23] Wang R, Ruan WH, Yang Q, Guo ZK, Cai RG, Hu B. Hubble parameter estimation via dark sirens with the lisa-taiji network. National Science Review. 2021 Apr;p. nwab054. https://doi.org/10.1093/nsr/nwab054.

[24] Wang G, Ni WT, Han WB, Xu P, Luo Z. Alternative LISA-TAIJI networks. Physical Review D. 2021 Jul;104(2):024012. https://doi.org/10.1103/PhysRevD.104.024012.

[25] The Taiji Scientific Collaboration. China's first step towards probing the expanding universe and the nature of gravity using a space borne gravitational wave antenna. Communications Physics. 2021 Dec;4(1):34. https://doi.org/10.1038/s42005-021-00529-z.

[26] Moore P, Turner JF, Qiang Z. Champ orbit determination and gravity field recovery. Advances in Space Research. 2003 Apr;31(8):1897–1903. https://doi.org/10.1016/S0273-1177(03)00164-9.

[27] Naeimi M, Flury J, editors. Global Gravity Field Modeling from Satellite-to-Satellite Tracking Data. Lecture Notes in Earth System Sciences. Cham: Springer International Publishing; 2017. Available from: http://link.springer.com/10.1007/978-3-319-49941-3.

[28] Reigber C, editor. Earth observation with CHAMP: results from three years in orbit. Berlin ; New York: Springer; 2005. Meeting Name: CHAMP Science Meeting.

[29] O'Keefe JA. An application of Jacobi's integral to the motion of an earth satellite. The Astronomical Journal. 1957 Oct;62:265. https://doi.org/10.1086/107530.

[30] Hotine M, Morrison F. First integrals of the equations of satellite motion. Bulletin géodésique. 1969 Mar;91(1):41–45. https://doi.org/10.1007/BF02524844.

[31] Wolff M. Direct measurements of the Earth's gravitational potential using a satellite pair. Journal of Geophysical Research. 1969 Oct;74(22):5295–5300. https://doi.org/10.1029/JB074i022p05295.

[32] Jekeli C. The determination of gravitational potential differences from satellite-to-satellite tracking. Celestial Mechanics and Dynamical Astronomy. 1999;75:85–101.

[33] Visser PNAM, Sneeuw N, Gerlach C. Energy integral method for gravity field determination from satellite orbit coordinates. Journal of Geodesy. 2003 Jun;77(3-4):207–216. https://doi.org/10.1007/s00190-003-0315-8.

[34] Jacobi JCG. Uber ein neues Integral f¨ur den Fall der drei K¨orper, wenn die Bahn des st¨orenden Planeten kreisf¨ormig angenommen und die Masse des gest¨orten vernachl¨assigt wird. Monthly Reports of the Berlin Academy of Science. 1836;July.

[35] Gerlach C, Sneeuw N, Visser P, Svehla D. CHAMP gravity field recovery using the energy balance approach. Advances in Geosciences. 2003 Jun;1:73–80. https://doi.org/10.5194/adgeo-1-73-2003.

[36] Gerlach C, Foldvary L, Svehla D, Gruber T, Wermuth M, Sneeuw N, et al. A CHAMP-only gravity field model from kinematic orbits using the energy integral. Geophysical Research Letters. 2003 Oct;30(20):2003GL018025. https://doi.org/10.1029/2003GL018025.

[37] Foldvary L, Svehla D, Gerlach C, Wermuth M, Gruber T, Rummel R, et al. Gravity Model TUM-2Sp Based on the Energy Balance Approach and Kinematic CHAMP Orbits. In: Reigber C, Lühr H, Schwintzer P, Wickert J, editors. Earth Observation with CHAMP. Berlin/Heidelberg: Springer-Verlag; 2005. p. 13–18. Available from: http://link.springer.com/10.1007/3-540-26800-6_2.

[38] Jaggi A, Bock H, Prange L, Meyer U, Beutler G. GPS-only gravity field recovery with GOCE, CHAMP, and GRACE. Advances in Space Research. 2011 Mar;47(6):1020–1028. https://doi.org/10.1016/j.asr.2010.11.008.

[39] Min J, Lei JG, Li YP, Xi DX, Tao WZ, Li CH, et al. Performance tests and simulations for Taiji-1 inertial sensor. International Journal of Modern Physics A. 2021 Apr;36(11n12):2140011. https://doi.org/10.1142/S0217751X2140011X.

[40] Peng X, Jin H, Xu P, Wang Z, Luo Z, Ma X, et al. System modeling in data processing of Taiji-1 mission. International Journal of Modern Physics A. 2021 Apr;36(11n12):2140026. https://doi.org/10.1142/S0217751X21400261.

[41] Pavlis NK, Holmes SA, Kenyon SC, Factor JK. The development and evaluation of the Earth Gravitational Model 2008 (EGM2008): THE EGM2008 EARTH GRAVITATIONAL MODEL. Journal of Geophysical Research: Solid Earth. 2012 Apr;117(B4):n/a–n/a. https://doi.org/10.1029/2011JB008916.

[42] Petit G, Luzum B. IERS Conventions (2010). International Earth Rotation and Reference Systems Service; 2011. No. 36. Available from: https://apps.dtic.mil/sti/citations/ADA535671.

[43] Folkner WM, Williams JG, Boggs DH. The Planetary and Lunar Ephemeris DE 421; 2009. vol. 42-178, p. 1-34.

[44] Dobslaw H, Bergmann-Wolf I, Dill R, Poropat L, Thomas M, Dahle C, et al. A new high-resolution model of non-tidal atmosphere and ocean mass variability for de-aliasing of satellite gravity observations: AOD1B

RL06. Geophysical Journal International. 2017 Oct;211(1):263–269. https://doi.org/10.1093/gji/ggx302.

[45] Picone JM, Hedin AE, Drob DP, Aikin AC. NRLMSISE-00 empirical model of the atmosphere: Statistical comparisons and scientific issues: TECHNIQUES. Journal of Geophysical Research: Space Physics. 2002 Dec;107(A12):SIA 15–1–SIA 15–16. https://doi.org/10.1029/2002JA009430.

[46] Wielicki BA, Barkstrom BR, Baum BA, Charlock TP, Green RN, Kratz DP, et al. Clouds and the Earth's Radiant Energy System (CERES): algorithm overview. IEEE Transactions on Geoscience and Remote Sensing. 1998;36(4):1127–1141.

[47] Wielicki BA, Wong T, Loeb N, Minnis P, Priestley K, Kandel R. Changes in Earth's albedo measured by satellite. Science. 2005;308(5723):825–825.

[48] Weigelt M, Dam T, Jaggi A, Prange L, Tourian MJ, Keller W, et al. Time-variable gravity signal in Greenland revealed by high-low satellite-to-satellite tracking. Journal of Geophysical Research: Solid Earth. 2013 Jul;118(7):3848–3859. https://doi.org/10.1002/jgrb.50283.

[49] Mayer-Gurr T, Ilk KH, Eicker A, Feuchtinger M. ITG-CHAMP01: a CHAMP gravity field model from short kinematic arcs over a one-year observation period. Journal of Geodesy. 2005 Mar;78(7-8):462–480. https://doi.org/10.1007/s00190-004-0413-2.

[50] Han SC, Jekeli C, Shum CK. Efficient gravity field recovery using in situ disturbing potential observables from CHAMP: GRAVITY FIELD RECOVERY FROM CHAMP. Geophysical Research Letters. 2002 Aug;29(16):36–1–36–4. https://doi.org/10.1029/2002GL015180.

[51] Badura T, Sakulin C, Gruber C, Klostius R. Derivation of the CHAMP-only global gravity field model TUG-CHAMP04 applying the energy integral approach. Studia Geophysica et Geodaetica. 2006 Jan;50(1):59–74. https://doi.org/10.1007/s11200-006-0002-3.